

Gaps and excitations in fullerides with partially filled bands : NMR study of Na_2C_{60} and K_4C_{60}

V. Brouet, H. Alloul

Laboratoire de Physique des Solides, Université Paris-Sud, Bat 510 91405 Orsay (France)

S. Garaj, L. Forró

*Laboratoire des solides semicristallins, IGA-Département de Physique,
Ecole Polytechnique Fédérale de Lausanne, 1015 Lausanne (Switzerland)*

(Dated: February 1, 2008)

We present an NMR study of Na_2C_{60} and K_4C_{60} , two compounds that are related by electron-hole symmetry in the C_{60} triply degenerate conduction band. In both systems, it is known that NMR spin-lattice relaxation rate ($1/T_1$) measurements detect a gap in the electronic structure, most likely related to singlet-triplet excitations of the Jahn-Teller distorted (JTD) C_{60}^{2-} or C_{60}^{4-} . However, the extended temperature range of the measurements presented here (10 K to 700 K) allows to reveal deviations with respect to this general trend, both at high and low temperatures. Above room temperature, $1/T_1$ deviates from the activated law that one would expect from the presence of the gap and saturates. In the same temperature range, a lowering of symmetry is detected in Na_2C_{60} by the appearance of quadrupole effects on the ^{23}Na spectra. In K_4C_{60} , modifications of the ^{13}C spectra lineshapes also indicate a structural modification. We discuss this high temperature deviation in terms of a coupling between JTD and local symmetry. At low temperatures, $1/T_1 T$ tends to a constant value for Na_2C_{60} , both for ^{13}C and ^{23}Na NMR. This indicates a residual metallic character, which emphasizes the proximity of metallic and insulating behaviors in alkali fullerides.

PACS numbers:

I. INTRODUCTION

Early after the discovery of fullerides, A_4C_{60} has been found to behave as an insulator rather than the metal expected in a band picture¹. The first indication for this was the detection by μSR in K_4C_{60} of a muonium precession² at 5 K, which is known to be quickly suppressed in presence of unpaired electrons. This signal disappears at higher temperatures suggesting the presence of thermally populated states. This has been confirmed by subsequent measurements of magnetic properties, ESR detects an activated susceptibility in K_4C_{60} with $E_a = 60 \text{ meV}^3$ and SQUID in Rb_4C_{60} yields $E_a = 60 \text{ meV}^4$. An activated component has also been found in NMR $1/T_1$ in K_4C_{60} with $E_a = 55 \text{ meV}^5$ and Rb_4C_{60} with $E_a = 70 \text{ meV}^{6,7}$. Other measurements also suggest an insulating ground state, no Fermi edge is visible by photoemission in K_4C_{60} and Rb_4C_{60} films⁸ and no Drude peak is found by optical conductivity⁹. However, in this latter study, the gap to the lowest conductivity peak is significantly larger than in magnetic measurements, around 500 meV. A more recent investigation by EELS in transmission¹⁰ also revealed a gap of the order of 500 meV in K_4C_{60} and Rb_4C_{60} . Therefore, two different gaps are necessary to describe these systems, a small “spin-gap” of the order of 50-100 meV and a larger “optical” gap of about 500 meV. As no magnetism has ever been reported at low temperature, the ground state for C_{60}^{4-} must be singlet and the small gap has been associated to singlet-triplet transitions^{6,7,11}. The large gap is presumably a direct gap in the substructure of the band. In addition, these systems are close to a metal-insulator

transition, as shown by the transition to a metallic state observed by NMR at 12 kbar in Rb_4C_{60} ⁷ and by the fact that the system with the smallest C_{60} - C_{60} distance, Na_4C_{60} , might even be metallic in its monomer phase ($T > 500\text{K}$), namely a body centered tetragonal (*bct*) structure^{12,13}, isostructural to other A_4C_{60} systems¹⁴.

Understanding the origin of the insulating state is a necessary step to describe the physics of fullerides. Although the crystal field due to the *bct* structure is not sufficient to lift the threefold degeneracy of the t_{1u} band (the C_{60} lowest unoccupied molecular orbital, filled with electrons brought by the alkali ions)¹, it has been suggested that this particular structure might explain why A_4C_{60} is insulating contrary to the metallic and face cubic centered (*fcc*) A_3C_{60} compounds¹⁵. Especially, the *bct* lattice is bipartite (contrary to the *fcc* one) which could play a role by enhancing antiferromagnetic correlations, hence favoring a Mott insulating state. However, we have shown recently that Na_2C_{60} , which is cubic¹⁶, exhibits a behavior similar to A_4C_{60} , with an activated temperature dependence of the NMR $1/T_1$ ¹¹. Electron-hole symmetry then applies in the t_{1u} band and the detection of a gap is an intrinsic feature of fullerides with 2 or 4 electrons per ball rather than one of the *bct* structure. The discrepancy with band structures must be sought in an underestimation of the role of electron-electron and/or electron-phonon interactions. The fact that these two interactions are strong and have similar orders of magnitude is actually one of the most interesting aspect of the physics of fullerides. This paper is a first of a serie of three papers (called hereafter I, II¹⁷ and III¹⁸), whose purpose is to present an extensive NMR study of different

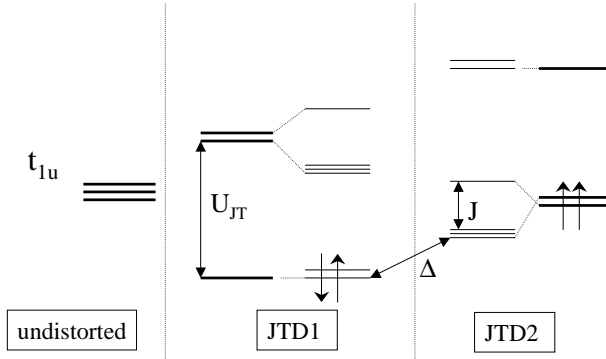


FIG. 1: Schematic representation of the structure of the three t_{1u} levels for two electrons per C_{60} and for the two most stable distortions (called JTD 1 and JTD 2) without spin degeneracy (thick lines) and with spin degeneracy (thin lines). The various gaps are indicated by arrows, the Jahn-Teller splitting U_{JT} , the exchange splitting J and the singlet-triplet gap Δ (adapted from ref.¹⁹).

stoichiometries to clarify this point.

There is a growing consensus that Jahn-Teller distortions (JTD) of the C_{60} molecule are an essential ingredient for the insulating state of A_4C_{60} , although they have never been detected directly in these compounds¹³. Molecular calculations¹⁹ indicate that the two most stable JTD correspond to the squeezing or elongation of the C_{60} molecule around one of the 3 equivalent axes of the quasi-spherical structure. This lifts the degeneracy of the t_{1u} levels by an amount of $U_{JT} \approx 0.5$ eV, as sketched on Fig. 1. The most stable JTD corresponds to a singlet ground state for C_{60}^{2-} (see the case JTD 1 on Fig. 1) and C_{60}^{4-} (case JTD 2), as observed experimentally. The first excited state of a C_{60}^{2-} is a triplet corresponding to JTD 2. It lies about $\Delta = 100$ meV higher in energy, which is consistent with the experimentally measured “spin-gap”.

In the solid, two different situations could occur, either a cooperative JT distortion or independent (and possibly dynamic) JT for each molecule. In the first case, a band gap could open if the cooperative JT is commensurate with the lattice. The second scenario is considered to be the most likely for fullerenes due to the unusually large quantum fluctuations on the C_{60} molecule^{20,21}. Another kind of excitation could take place between the t_{1u} levels split by the JTD, and $U_{JT} = 500$ meV would correspond to the large “direct” optical gap. Let us emphasize that as U_{JT} has the same order of magnitude as the band width W , so that the gap in other directions should be much smaller. This is why Fabrizio *et al.* have proposed that strong electronic correlation combined with JT are necessary to understand the insulating state, which could be called a “Mott Jahn-Teller” ground state²⁰. As we have seen, this model is supported by the large body of experiments in Na_2C_{60} and A_4C_{60} , because it explains the occurrence of two gaps and predicts correct order of magnitude for them.

In this paper, we will first introduce the basic NMR

facts indicating that Na_2C_{60} and K_4C_{60} are insulators with similar properties and in good agreement with the “Mott JT model” described previously (section II). We then present data up to very high temperatures (700 K) that call for a more refined model than a simple thermal population of an excited state. We suggest in section III that subtle changes in local symmetry detected by NMR near room temperature could be a relevant parameter to explain the high temperature evolution of the physical properties. The structural modifications likely couple to the JTD and might modify the equilibrium between singlet and triplet states. In the last section, we will study in details the question of a possible coexistence of metallic behavior in Na_2C_{60} with the aforementioned molecular excitations. As explained previously, this is not inconsistent with the “Mott JT scenario” and the status of JTD in a metallic or semimetallic environment is actually an important issue to clarify.

II. A NON-MAGNETIC GROUND STATE WITH GAPPED EXCITATIONS

In this section, we show that the ^{13}C NMR spectra shifts and lineshapes, as well as the dynamic susceptibility monitored by the spin lattice relaxation rate $1/T_1$, exhibit similar features in Na_2C_{60} and K_4C_{60} . Both compounds are characterized by a non-magnetic ground state and a gap in their low-energy excitations. We present new measurements above room temperature that allow to investigate this behavior in more details.

A. ^{13}C NMR spectra

Let us detail first that the evolution of the ^{13}C NMR spectra at low temperatures, shown on Fig. 2, clearly demonstrates that no magnetic transition occurs in Na_2C_{60} and K_4C_{60} . To understand this, let us first recall the interactions contributing to the shift K of one NMR line.

$$\overline{\overline{K}} = \overline{\overline{\sigma}} + \overline{\overline{A}} \overline{\overline{\chi}} \quad (1)$$

$\overline{\overline{\sigma}}$ represents a chemical shift tensor and $\overline{\overline{A}} \overline{\overline{\chi}}$ the contribution from unpaired electrons called Knight shift. $\overline{\overline{A}}$ is the hyperfine coupling tensor between ^{13}C and unpaired electrons and χ the local electronic susceptibility. All these quantities have both isotropic and anisotropic parts. In the case of C_{60} compounds, the anisotropic part is usually the largest because electrons reside mainly in orbitals with a pronounced p character. As these orbitals have nodes at the nuclear position, the electrons do not interact directly with the ^{13}C nuclear spin through the so-called contact interaction and the hyperfine coupling is mainly of dipolar origin²². As a consequence, the shift is a function of the orientation of one orbital with respect

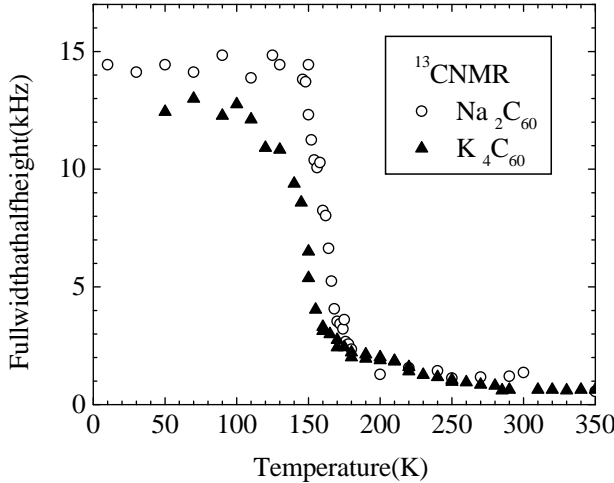


FIG. 2: ^{13}C NMR linewidth as a function of temperature for Na_2C_{60} and K_4C_{60} . The broadening of the spectra due to the slowing down of the C_{60} molecular motions is visible around 150 K.

to the NMR applied field. At high temperatures, when the molecules are rapidly rotating, the anisotropic contribution is averaged out and narrow lines are observed. They broaden when the motions slow down and appear static on the NMR time scale (a few ms). This has been observed in many fullerenes and Fig. 2 shows that this takes place at 150 K in the case of K_4C_{60} and 160 K for Na_2C_{60} . We note that the timescale of the C_{60} motion appears to be similar in both compounds, despite the different structures and presumably different interactions between C_{60} and K or Na.

There is no further broadening of the spectra below this temperature, which means that there is *no magnetic transition* at least down to the lowest measured temperature, 10 K in Na_2C_{60} and 50 K in K_4C_{60} . Indeed, static magnetic moments would create a large local magnetic field on ^{13}C nuclei and cause a large broadening of the spectra in these powder samples. This finding is one key element to involve Jahn-Teller distortions in the description of these materials because they explain naturally the singlet ground state. Otherwise, one could have rather expected a magnetic ground state for localized electrons, because Hund's rule should favor a high spin state in the t_{1u} levels.

Relevant information about the insulating state should be found in the temperature dependence of the static spin susceptibility, that could in principle be extracted from the isotropic part of the Knight shift. Fig. 3 shows that this is difficult because the isotropic shift (defined as the center of gravity of one spectrum) is small with respect to the linewidth, especially at low temperature. In pure C_{60} , an isotropic chemical shift $\sigma = 143$ ppm is observed²³, characteristic of the orbital currents flowing in the filled orbitals. This is expected to be the order of magnitude of the reference for the Knight shift in alkali fullerenes. This idea was confirmed by the close value

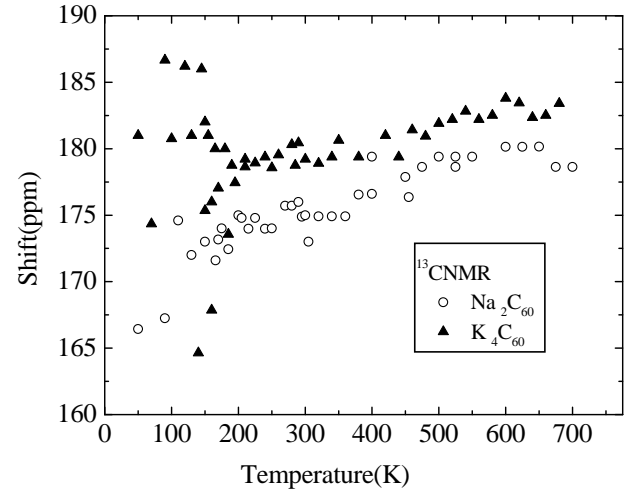


FIG. 3: Temperature dependence of the shift (with respect to TMS) of the center of gravity of the ^{13}C NMR spectra in Na_2C_{60} and K_4C_{60} . The accuracy is lower at low temperatures because of the broadening of the spectra.

of 156 ppm found in the band insulator A_6C_{60} ²⁴, which suggests an empirical correlation for σ of +1.5 ppm per added electron. In K_4C_{60} and Na_2C_{60} , the shifts are however much larger than what would be expected with such a contribution for σ alone. At room temperature $K = 175$ ppm for Na_2C_{60} and 179 ppm in K_4C_{60} , which is comparable to shifts measured in metallic A_3C_{60} (189 ppm in K_3C_{60} for example²⁵). This sizable Knight shift indicates the presence of electronic excitations giving rise to a large electronic susceptibility at room temperature.

At low temperature, the anisotropic part of the shift, which is also proportional to the susceptibility, can be studied as well. Typical ^{13}C lineshapes are presented on Fig. 4, they are similar in Na_2C_{60} and K_4C_{60} with a shoulder on the low frequency side, characteristic of the chemical shift anisotropy found in pure C_{60} ²³. This can be stated more quantitatively if one extracts the parameters for the shift tensor by fitting the spectra to the theoretical powder pattern²⁶. Defining,

$$K = K_{iso} + K_{ax} \left(\frac{3 \cos^2 \theta - 1}{2} \right) + K_{asym} \sin^2 \theta \cos 2\varphi \quad (2)$$

where θ and φ are the spherical coordinate for the orientation of the principal axis of the tensor with respect to the applied magnetic field, one can compute the actual lineshape by averaging on all possible orientations. The values found for Na_2C_{60} and K_4C_{60} are reported on Fig. 4, together with the fit of the experimental spectra. A convolution with a gaussian function of width 35 ppm has been used to take into account an experimental broadening and reproduce the spectra. Because the parameters are not independent, we estimate an error ± 5 ppm for each of them. K_{ax} and K_{asym} are very similar to the parameters found in pure C_{60} ($K_{ax} = -110$

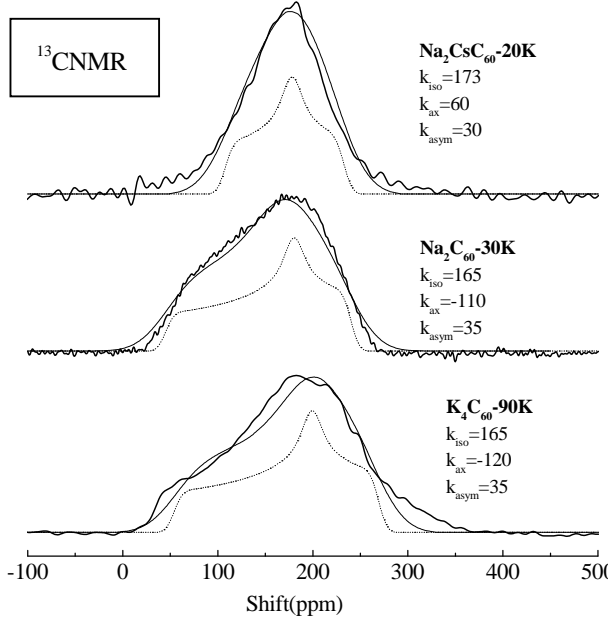


FIG. 4: ^{13}C NMR spectra at low temperatures for K_4C_{60} , Na_2C_{60} and $\text{Na}_2\text{CsC}_{60}$ (thick lines). Fit to a powder pattern of the anisotropic NMR shift (Eq. 2) are also presented with parameters indicated on the figure. The thin solid line is obtained by a convolution of the theoretical lineshape with a gaussian of half width at half maximum 35 ppm. A convolution with a 10 ppm large gaussian is also shown (dotted line) that reveals more clearly the underlying structure of the spectra.

ppm and $K_{\text{asym}} = 35$ ppm²³) even though the spectra are shifted by about 20 ppm. In contrast, it has been observed that for metallic A_3C_{60} compounds, the addition of the Knight shift anisotropy leads to *narrower* and more *symmetric* lines. This is illustrated by the spectra in $\text{Na}_2\text{CsC}_{60}$ also shown on the figure. Therefore, the observation of the typical C_{60} lineshape in Na_2C_{60} and K_4C_{60} is a sign that the contribution of conduction electrons is weak at low temperature. The relatively large value found for the isotropic coupling ($K=165$ ppm) might be due to a slightly larger value of σ than the one estimated previously.

The susceptibility then increases from a small value at low T to a sizable one at room temperature, which is consistent with the presence of singlet-triplet excitations in these compounds proposed in the introduction. We will see in the course of this paper that we can confirm the presence of these excitations more accurately using other NMR probes.

B. ^{13}C NMR spin-lattice relaxation

1. Detection of a gap in the electronic structure

The most efficient way to detect these excitations is through spin-lattice relaxation measurements ($1/T_1$), which measures the imaginary part of the electronic susceptibility, that is, if no particular q dependence is expected.

$$\frac{1}{T_1} = \frac{k_B T}{\hbar} A^2 \frac{\chi''(\omega_0)}{\omega_0} \quad (3)$$

As can be seen on Fig. 5, $1/T_1$ increases steeply with temperature for both compounds, the increase starts around 150 K in K_4C_{60} and 200 K in Na_2C_{60} . This has been observed previously (see ref.⁵ for K_4C_{60} and ref.¹¹ for Na_2C_{60}) and can be attributed to a gap related to singlet-triplet transitions between two different JTD, as explained in the introduction. The lines on Fig. 5 correspond to activated laws with $E_g = 70$ meV for K_4C_{60} and $E_g = 140$ meV for Na_2C_{60} and they describe the data correctly up to room temperature. At higher temperature, deviations are observed, which will be discussed in the last paragraph of this section. In Rb_4C_{60} , the activated part of $1/T_1$ below 250 K is almost quantitatively identical to that of K_4C_{60} ⁷. This could mean that the 70 meV gap is characteristic of a JT C_{60}^{4-} , while it is nearly twice larger for C_{60}^{2-} . However, we will argue in this paper that the gap extracted from $1/T_1$ could be slightly different from the molecular value, because it is sensitive to the details of the local structure. Besides stoichiometry, one similarity between K_4C_{60} and Rb_4C_{60} that contrasts with Na_2C_{60} is precisely that they both have a *bct* structure and this could also be the reason for the different gaps in Na_2C_{60} and A_4C_{60} .

In a previous study⁵, Zimmer *et al.* have proposed a smaller gap in K_4C_{60} (50 meV), because they assign part of the increase of $1/T_1$ to a molecular motion peak. They suggested that $1/T_1$ would follow the dashed line of Fig. 5, once this peak is subtracted. By extending the measurement to higher temperature, we show that $1/T_1$ on the contrary *saturates* above 250 K towards $1/T_1 = \text{cst}$, which invalidates this analysis. As for a molecular motion peak, Fig. 5 shows that it is unambiguously resolved at 180 K for Na_2C_{60} , but it does not appear clearly for K_4C_{60} . In the next section, we study this contribution in more details, to determine to what extent it could modify the shape of $1/T_1$ vs T .

2. Realistic parameters for the molecular motion peak contribution

Indeed, molecular motions have been found to contribute to $1/T_1$ in different fullerides, most notably pure C_{60} ²³ and K_3C_{60} ²⁷. This is due to the fact that the local magnetic field H_{loc} sensed by ^{13}C nuclear spin depends

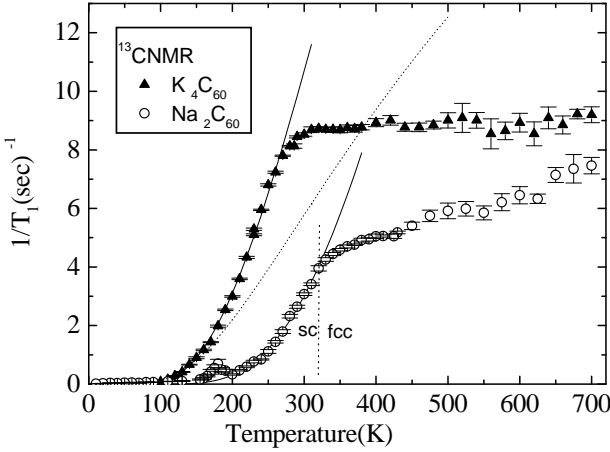


FIG. 5: ^{13}C NMR $1/T_1$ in Na_2C_{60} and K_4C_{60} from 10 to 700 K. Solid lines are fit to an activated law below room temperature. The dashed line for K_4C_{60} is an extrapolation of the electronic contribution to $1/T_1$ given in ref.⁵ based on data below 300 K and assuming a contribution from molecular motion peak.

on the orientation of the p_z orbital, nearly perpendicular to the C_{60} ball at one carbon site, with respect to the NMR applied field. Rotation of the ball will *modulate* this local field. If the timescale of the motions is such that they create fluctuations of H_{loc} at the nuclear Larmor frequency ω_0 , they can relax the NMR nuclei. For fullerides, the fast rotation of the C_{60} molecule around one axis can be described by a frequency $1/\tau$ that is typically of the order of ω_0 for temperatures around 200 K–400 K. A “Bloembergen Purcell Pound” peak²⁸ can be expected in this temperature range with :

$$\frac{1}{T_1} = \alpha (\gamma H_{loc})^2 \frac{2\tau}{1 + (\omega_0\tau)^2} \quad (4)$$

where γ the gyromagnetic ratio for the nuclei and α is a numeric prefactor of order unity, which depends on the details of the molecular motion.

To determine the actual value of α , the anisotropy of H_{loc} , measured from the low temperature spectra, should be used and the molecular motion should be modelled in an appropriate way, for example a uniaxial rotation along one diagonal axis, following the lines of²⁹. The maximum value of α is 1 if the local field is assumed to fluctuate randomly between two values $\pm H_{loc}$ ²⁶ but it can be much smaller, for example 6/40 in the case of random molecular reorientation for an axial symmetry of the shift tensor³⁰. Here, we want to estimate α from the experiment rather than from a theoretical model; to do so, some typical molecular contributions to $1/T_1$ are shown on Fig. 6.

From Eq. 4, it can be seen that the maximum of $1/T_1$ occurs for $\omega_0\tau = 1$ with a value *depending uniquely on the linewidth* $\Delta\nu = \gamma H_{loc}/2\pi$. It is given by $1/T_1)_{\max} = \alpha (\gamma H_{loc})^2/\omega_0$. We have shown in the preceding section that K_4C_{60} , Na_2C_{60} and C_{60} exhibit roughly the same

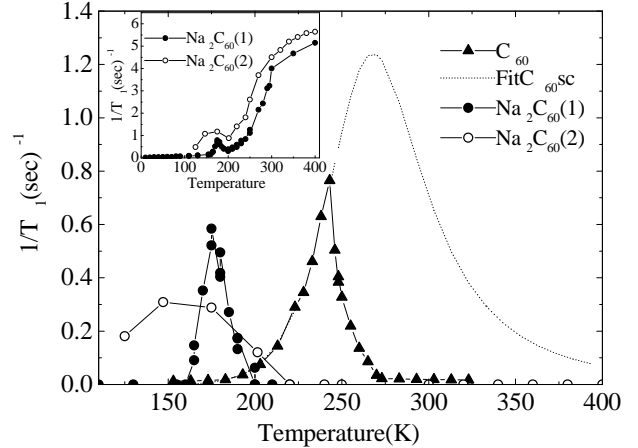


FIG. 6: Comparison of the molecular motion peak contribution to $1/T_1$ in pure C_{60} (ref.²³) and two Na_2C_{60} samples. The dashed line is a fit of the molecular motion in the *sc* phase of C_{60} ($T < 260$ K) given in ref.²³. Inset : $1/T_1$ as a function of temperature in the two Na_2C_{60} samples.

linewidth, so that similar contributions should be expected. Pure C_{60} is the simplest case because the relaxation is dominated by molecular motions and the field dependence predicted by Eq. 4 has been successfully checked³¹. The data from ref.²³ are reported on Fig. 6, and yield $1/T_1)_{\max} = 0.8 \text{ sec}^{-1}$. Let us note that these authors have extrapolated a “true” maximum $1/T_1)_{\max} = 1.2 \text{ sec}^{-1}$ (dashed line), assuming that the peak is “cut” by the orientational transition at 260 K. This order of magnitude is consistent with the peak $1/T_1)_{\max} = 0.6 \text{ sec}^{-1}$ found in Na_2C_{60} . When looking at Fig. 5, it is clear that a contribution of the order of 1 sec^{-1} would not severely affect our discussion of K_4C_{60} .

The width of the peak depends on the variation of τ with temperature and an Arrhenius law $\tau = \tau_0 \exp(E_a/T)$ is usually used, where E_a is the activation energy for the molecular motion and $1/\tau_0$ the attempt frequency. These parameters are probably similar for different compounds and a typical width of about 50 K can be deduced from Fig. 6. Interestingly, we have found a significant difference between two Na_2C_{60} samples, called (1) and (2) on Fig. 6. The results presented here are from sample (1), sample (2) exhibits a similar behavior but seems to be of somewhat poorer quality, as can be seen by the slightly shorter T_1 values (see inset of Fig. 6) or slightly broader linewidth. The molecular motion peak, although clearly present, is broader in sample (2), which is likely due to a distribution of the motion parameters, and consequently its maximum amplitude is smaller. Data on Fig. 5 imply that, if present, the peak in K_4C_{60} must be very broad, which could be due to sample quality or intrinsic disorder of the bct phase. Its intensity would be accordingly reduced, so that its contribution is furthermore negligible.

3. High temperature behavior

The $1/T_1 = cst$ law observed at high temperatures in K_4C_{60} is then intrinsic. It is somewhat unusual as most relaxation mechanisms give an increasing relaxation rate with increasing temperature. Such a flat behavior is reminiscent of the relaxation observed in dense paramagnets, which is caused by a coupling to localized paramagnetic centers. Within our model of singlet-triplet excitations of JTD balls, we do have such centers at high temperatures, namely the triplet states. Nevertheless, our first expectation would be to observe such a law only when the population of these levels saturates, for temperatures above the ST gap, i.e. $T > 800 K$. More correctly, as $1/T_1$ measures the imaginary part of the electronic susceptibility (see Eq. 3), it is sensitive to both the *nature* and the *dynamic* of the relevant electronic excitations. In our case, this means that both the number and the lifetime of the triplet states contribute to $1/T_1$, so that an abrupt change in the temperature dependence of one of this quantity could explain the change in $1/T_1$. In Na_2C_{60} , we observe a similar deviation from the activated law before the expected saturation for $T = Eg$, although it is not constant like in K_4C_{60} , but keeps increasing slightly up to 700 K. As the deviation is present in both systems, it must contain some insights of their physics.

The first possibility is that the activated law fails to describe the data over the full temperature range because there are other thermally accessible excitations, like for example the singlet state of JTD 2 in Fig. 1, if J is small enough. A variant of this idea is that the arrangement of the molecular levels could be modified with increasing temperature. JTD being sensitively coupled to the structure's crystal field, it is likely that even small structural modifications could affect the equilibrium between different JTD. A second possibility that goes beyond this "molecular approach", is related to the fact that we deal here with solids that are very close to a metal-insulator transition, where hopping is certainly not strictly forbidden. The introduction of an hopping term in the JT hamiltonian mixes different molecular states and can also affect the nature of the ground state. An estimation of the temperature dependence of the lifetime of the triplet state is obviously a complicated problem, as it probably involves both the dynamic of the Jahn-Teller distortion and hopping rates as a function of temperature. Nevertheless, if a static distortion is for example stabilized at low temperatures, allowing eventually the development of a cooperative distortion, it could certainly affect $1/T_1$.

In any case, the evolution of $1/T_1$ at high temperature cannot be understood with a model of isolated molecules and forces us to take into account interactions between the balls and/or with the structure. For Na_2C_{60} , it is for example suggestive that $1/T_1$ departs from the activated behavior near the temperature of the structural orientational transition taking place at 310 K¹⁶. In an attempt to identify the origin of the change in $1/T_1$, we now turn

our attention to details of the structure that can be studied by NMR to see whether there is any detectable change in the corresponding temperature range.

III. INTERPLAY BETWEEN JTD AND LOCAL SYMMETRY

There are very few cases where Jahn-Teller distortions have been observed directly in fullerenes. One example is C_{60} -tetraphenylphosphonium bromide, a salt where C_{60}^- molecules are well separated from each other. A cooperative Jahn-Teller state is thought to develop below 120 K, because a splitting of the Lande factor has been observed by ESR below 120 K³². Interestingly, a transition to an orientationally ordered state is observed at about the same temperature³³, so that it seems likely that the new orientational order stabilizes the collective distortion. This example motivates us to relate to structural modifications the particular evolution of $1/T_1$ at high temperatures. NMR, and especially alkali NMR, has proved to be a very sensitive probe for small structural distortions in fullerenes²². We first focus on the effect of the structural transition in Na_2C_{60} on the electronic properties, as seen by ^{23}Na NMR. We then review other signs of structural evolution in Na_2C_{60} and K_4C_{60} that indeed seem to coincide with the change in the electronic behavior.

A. Structural transition in Na_2C_{60} studied by ^{23}Na NMR

The analysis of the electronic properties of alkali fullerenes might be complicated by the structural modifications associated with orientational ordering or freezing of the molecular motions. Although such structural modification could appear minor at first sight, it has for example often be argued in the case of $n=3$ that *sc* phases behave quite differently from *fcc* phases³⁴. In the case of Na_2C_{60} the occurrence of an orientational transition at 310 K might then affect deeply the electronic properties. At least, it seems reasonable to assume that some parameters (such as the gap value) could be different on both sides of the transition. Fitting the temperature dependence of χ or $1/T_1$ then becomes more difficult.

This can be clarified by ^{23}Na NMR because ^{23}Na spectra differ in the two phases, which allows to discriminate what happens in the *sc* and *fcc* phases respectively. In the inset of Fig. 7, a spectrum at 310 K shows the co-existence of the two phases, which we observe from 300 K to 315 K. Following the shift of each line, as done in Fig. 7, we can extract the susceptibility in both phases independently and observe that χ increases in *both sc* and *fcc* phases. We also clearly see that a "saturation" appears in the *fcc phase* at 400K, and not at the structural transition. This contradicts the impression given by ^{13}C $1/T_1$, which seems to change at the structural transition,

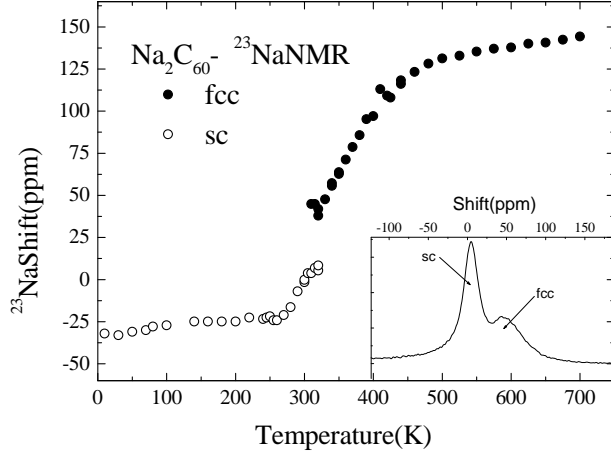


FIG. 7: ^{23}Na NMR shifts (with respect to NaCl) in Na_2C_{60} for the *fcc* phase (solid circles, $T > 310\text{K}$) and the *sc* phase (open circles). Inset : ^{23}Na spectrum at 310 K showing the coexistence of the two structures.

but this is more precise as ^{13}C NMR does not resolve two different signals and only the average value is accessible.

In the *fcc* phase, the scaling between K and the ESR susceptibility is excellent (see Fig. 8) and the hyperfine coupling A_{fcc} can be extracted using Eq. 1, provided that σ_{fcc} is temperature independent (which is a usual assumption). We obtain $\sigma_{\text{fcc}} = -65 \text{ ppm}$ and $A_{\text{fcc}} = 3500 \text{ Oe}/\mu_B$. The evolution of the susceptibility in the *sc* phase is especially interesting as the ESR susceptibility is masked by a large Curie term below 200 K. Following Eq. 1, the discontinuity at the transition could be attributed either to a different hyperfine coupling A or to a different susceptibility. The hyperfine coupling is defined by the local environment of a Na atom, which is indeed very different in *sc* or *fcc* phases. In the *fcc* phase, the orientations of the four neighboring C_{60} balls are such that Na faces four hexagonal rings, whereas, in the *sc* phase, it faces only one hexagonal ring and three double bonds (see ref.³⁵ and picture of Fig. 9). Therefore, there are probably two different hyperfine couplings A_{sc} and A_{fcc} . As ESR or ^{13}C $1/T_1$ do not exhibit any obvious discontinuity at the transition, χ is more likely to be continuous. Assuming that σ and χ do not change at the transition, we find $A_{\text{sc}} = 2300 \text{ Oe}/\mu_B$ and the variation of χ deduced from NMR is reported on Fig. 8 by open circles for *sc* phase.

We can now compare this refined estimation of χ to the singlet-triplet model. A first conclusion is that χ tends to a constant value at low temperatures corresponding to $\chi = 7.10^{-5} \text{ emu/mol}$. Although, this is somehow dependent on our assumption that $\sigma_{\text{sc}} = \sigma_{\text{fcc}}$, we have found a very similar value ($6 \cdot 10^{-5} \text{ emu/mol}$) when trying to compare directly T_1 and χ_{esr} in ref.¹¹, which gives some confidence in this estimate. This suggests the presence of a Pauli-like contribution in Na_2C_{60} , which likelihood will be discussed in the last section of this paper.

For the activated part, the singlet-triplet model of

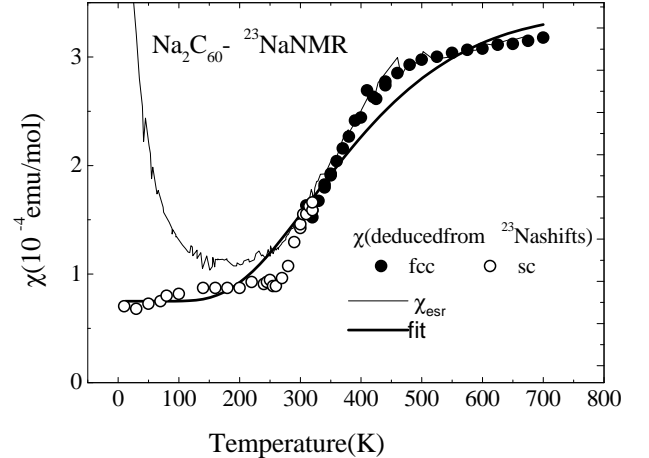


FIG. 8: ESR susceptibility measured on the same Na_2C_{60} batch than the NMR sample (thin line). Symbols represents an extrapolation of the true susceptibility extracted from ^{23}Na NMR shifts as explained in the text. The thick line is a fit to the model described in the text (Eq. 5).

Fig. 1 predicts a susceptibility $\chi(T) = n(T) * \chi(S_1)$, where $n(T)$ is the number of thermally populated triplet states and $\chi(S_1)$ the Curie susceptibility for triplet states.

$$\chi(T) = \frac{3 \exp(-\Delta/T)}{2 + 3 \exp(-\Delta/T)} * \frac{8\mu_B^2}{3k_B T} \quad (5)$$

The thick line on Fig. 7 is a fit to such a relation with $\Delta = 100 \text{ meV}$, which is 25 % smaller than by using the estimation based on $1/T_1$ data below room temperature. Quantitatively, the measured susceptibility corresponds to 80 % of that estimated by Eq. 5, which sounds reasonable. Although this law clearly captures much of the physics of this phase, it does not fit satisfactorily our data over the whole T range. We observe a steeper increase of the susceptibility at 250 K and a larger inflection at 450 K. This suggests that “something else” might come into play at these temperatures, that helps or hinders the population of triplet states, and that it is not purely a thermal process. One of the possibility that comes into mind is a small structural modification that would stabilize a particular state.

B. Quadrupole effects on ^{23}Na in Na_2C_{60}

If the orientational structural transition does not seem to modify deeply the behavior of Na_2C_{60} , we present here the observation of further changes in local symmetry happening in the *sc* phase that could couple to Jahn-Teller distortions and interact with the electronic properties.

As ^{23}Na is a spin $3/2$, it is sensitive to electric field gradients (EFG) arising from deviations from cubic symmetry at the Na site. In the *fcc* phase, there are no detectable quadrupole effects, as expected in the cubic

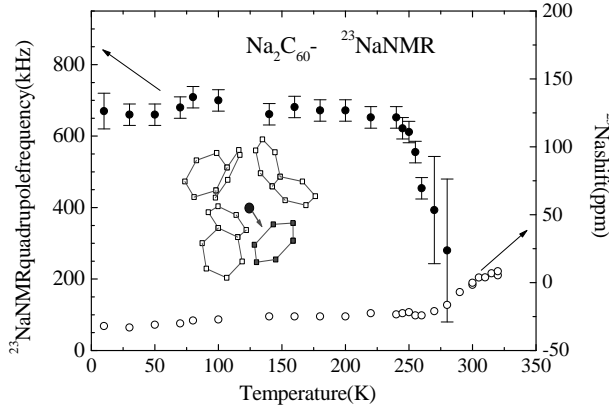


FIG. 9: Structural distortion in Na_2C_{60} evidenced by the appearance of a nuclear quadrupole frequency in the ^{23}Na spectra below 250 K (solid points, right scale). The picture suggests that the distortion is due to a displacement of Na towards the hexagon of one of its four C_{60} neighbor. Left scale : ^{23}Na NMR shift that starts increasing when the quadrupole frequency disappears.

environment of one tetrahedral site. However, in the *sc* phase, a decrease in the NMR intensity at the *fcc* to *sc* transition indicates that quadrupole effects are present. In this case, the $(-3/2 \rightarrow -1/2)$ and $(1/2 \rightarrow 3/2)$ nuclear transitions are wiped out of the spectrum and only the central nuclear transition $(1/2 \rightarrow -1/2)$ is detected. Below 200 K, a splitting of this central transition, which is characteristic of second order broadening by the EFG³⁰ is detected. The $(1/2 \rightarrow -1/2)$ line can be fitted at 100 K by an EFG tensor with a quadrupole frequency $\nu_q = 700$ kHz and a small asymmetry $\eta = 0.2$ ³⁶. The evolution of ν_q with temperature is displayed on Fig. 9, it shows that this quadrupole effect progressively increases when the temperature is lowered from 280 to 230 K.

Where does this EFG come from ? As represented on Fig. 9, in the *sc* phase, the environment of ^{23}Na is quite asymmetric. This could favor a displacement of Na along the cube diagonal (indicated by the arrow) towards the hexagonal ring, as was observed by x-ray in the structurally similar $\text{Na}_2\text{CsC}_{60}$ ³⁵, that would create an electric field gradient. C_{60} molecular motions have to be reduced to allow this displacement. More precisely, rotation around one axis could still exist (and it probably persists down to about 180 K where we observe the peak in ^{13}C NMR $1/T_1$) but reorientation of the rotation axis must be nearly prohibited (such a decomposition of the molecular motion was proposed for K_3C_{60} ²⁷). Here, we believe that this “slow” reorientational motion is slowing down progressively when we begin to observe static quadrupole effects around 280 K and is totally frozen below 250 K.

It is quite striking that the ^{23}Na shift, plotted again on Fig. 9 for comparison, starts to increase just as the EFG disappears and this strongly suggests a relation between the two effects. One possibility is that this increase reflects the one of the hyperfine coupling as the

Na atom moves because of the distortion. However, we have seen in the previous section that the shift can be rather well understood in terms of a singlet-triplet susceptibility, so that we believe that it is the susceptibility that starts to increase suddenly when the distortion disappears. This indeed would explain the steeper increase of the shift compared to the singlet-triplet model noted on Fig 8. This suggests that the distortion stabilizes the singlet state and that triplet states can only be significantly populated when it disappears. The exact microscopic origin of such an interplay is not yet clear. The orbital moment of the triplet distortion might be incompatible with the crystal field induced by the structural distortion, which forbids their existence.

C. Change of the symmetry of the C_{60} molecular motion in K_4C_{60}

In K_4C_{60} , there is no ordering transition but we report here in Fig. 10 modifications of the ^{13}C lineshape that indicate a structural evolution. At high temperatures, the ^{13}C spectrum consists of one narrow symmetric line, as expected because of the motional narrowing of the spectrum. However, a shoulder appears below 580 K on the low frequency side, and becomes progressively better defined as the temperature is lowered. This lineshape is characteristic of a small axial anisotropy and probably corresponds to the development of the uniaxial motion, which would not be completely averaged anymore by molecular reorientations. Note that this anisotropy is however still very small with respect to the low temperature one (200 ppm). Below 250 K, the spectral weight is quite suddenly transferred to the right of the spectra, as noted on the figure by the appearance of a “peak 2” and “shoulder 2”. Fig. 11 summarizes the situation by displaying the shift of the various peaks as a function of temperature. This complex behavior is not understood,

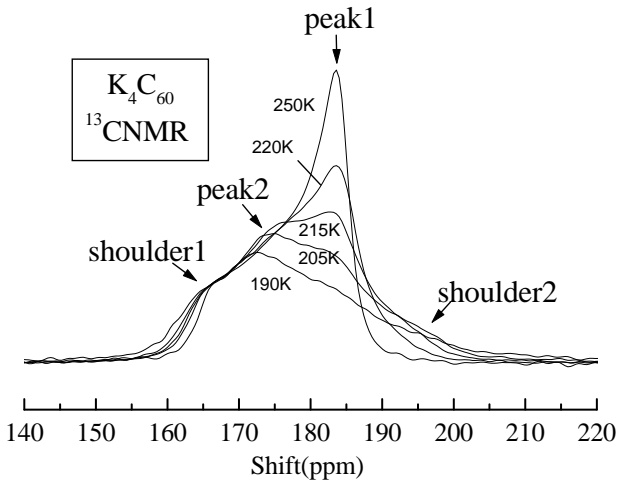


FIG. 10: ^{13}C NMR spectra in K_4C_{60} from 190 K to 250 K showing a change in the ^{13}C lineshape.

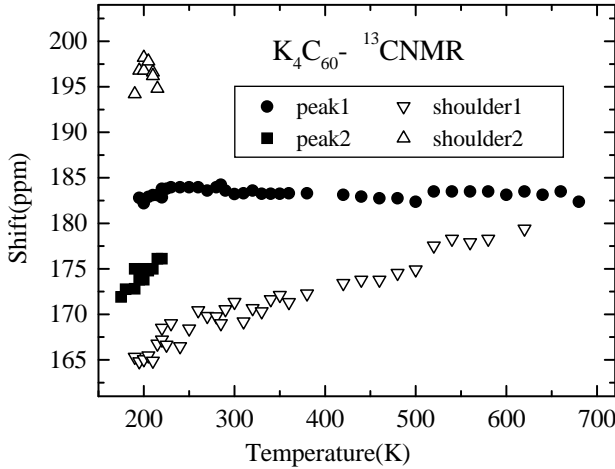


FIG. 11: Shifts of the different peaks indicated on Fig. 10 in the ^{13}C NMR spectrum of K_4C_{60} from 200 to 700 K.

but it is probably related to a change in the symmetry of the molecular motion. This shows that, even though there is no reported structural transition in K_4C_{60} in this temperature range, the local symmetry changes. Let us recall that a true structural transition has been detected by differential thermal analysis in K_3C_{60} at 200 K that has never been associated so far to a precise structural deviation²⁷.

As a matter of fact, $1/T_1$ saturates precisely in this temperature range, as can be checked on Fig. 5. This “coincidence” bears some similarity with the case of Na_2C_{60} , which incites us to take it seriously. When discussing the $1/T_1 = \text{cst}$ regime, we mentioned that it could be understood by a coupling to a fixed number of triplet states. This would require that the structural change at 250 K favors the triplet states almost exclusively.

Very recently an infrared study of K_4C_{60} has revealed a splitting of the two high frequency T_{1u} modes from a doublet above 250 K to a triplet at lower temperature³⁷. This observation definitely establishes a symmetry breaking in this temperature range, although the exact nature of the JTD and their ordering in the high and low temperature phases is still unclear.

IV. COEXISTENCE WITH A METALLIC CHARACTER?

So far, our study has been mainly focused on the molecular singlet-triplet excitations that dominate the high temperature behavior. However, we have seen that a Pauli-like contribution seems to be present in χ for Na_2C_{60} , which could imply that Na_2C_{60} is weakly metallic. Such a possible coexistence of band-like excitations with typically molecular ones is an important issue. It could indeed help to clarify the nature of the metal-insulator transition in A_nC_{60} . Two different kind of such transitions could be considered, the one that takes place

in Rb_4C_{60} as a function of lattice spacing, which has been observed under applied pressure⁷ and the one expected as a function of doping if one could go continuously from Na_2C_{60} to A_3C_{60} to A_4C_{60} . Therefore, we pay hereafter particular attention to this subject by studying the low temperature behavior of $1/T_1$ in Na_2C_{60} , which probes the nature of the excitations of the ground state of this system.

The temperature dependence of $1/T_1 T$ at low T in Na_2C_{60} and K_4C_{60} is emphasized in the logarithmic plot of Fig. 12. It can be seen that in Na_2C_{60} , $1/T_1$ deviates from the activated behavior below 100 K, actually $1/T_1 T$ tends to a constant value for ^{13}C and ^{23}Na . On the other hand, in K_4C_{60} , $1/T_1 T$ follows the activated law of Fig. 5 down to the lowest measured temperature. The very long value for T_1 in this system at this temperature prevents us to study this behavior further. In Rb_4C_{60} also, the low temperature data do not follow the activated behavior but was ascribed to a much smaller gap (10 meV)⁷. As $1/T_1 T = \text{cst}$ is the Korringa law expected in a metal, this reinforces the possibility of a weak metallicity of Na_2C_{60} . Before concluding firmly on this eventuality, we have to consider possible complications in the interpretation of the relaxation data.

A. Relaxation curves

To be sure of the temperature dependence of $1/T_1$ down to the lowest temperature, one has to check first that the shape of the nuclear magnetization recovery curve after saturation is not changing. This question is not trivial in fullerenes as a non-exponentiality always appears at low temperatures, giving some ambiguity in the actual definition of an average T_1 value. In Na_2C_{60} and K_4C_{60} , this happens below 150 K, but Fig. 13 shows that the relaxation curves can be *scaled together* for different temperatures. This means that they keep a similar shape

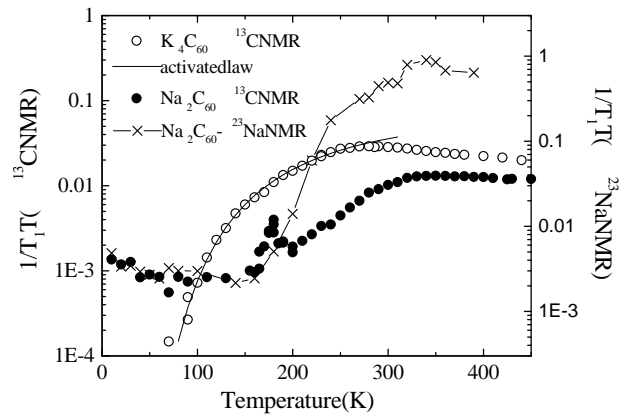


FIG. 12: Comparison of $1/T_1 T$ for ^{13}C and ^{23}Na in Na_2C_{60} and ^{13}C in K_4C_{60} as a function of temperature. Note the logarithmic scale. The solid line is the activated law of Fig. 5 for K_4C_{60} .

with varying temperature within experimental accuracy, and therefore a single time parameter which is taken as T_1 can be used to characterize the variation of the relaxation below 150 K. The actual value of T_1 somehow depends on the expression used to fit the magnetization recovery curve but not its temperature dependence.

In Na_2C_{60} , the relaxation curves can be described by a stretched exponential $M(t) = \exp((-t/T_1)^\beta)$ with values of β ranging from 0.5 to 0.6. Within experimental accuracy, many different laws could describe this dependence, from multi-exponential recovery (2 sites or more) to stretched exponential. We choose the latter not for physical reasons but because it allows to compare easily the relaxation in different systems. The same fit applies in K_4C_{60} , although the experimental accuracy is not sufficient to determine β very precisely. All the curves presented on Fig. 13 are fitted with $\beta = 0.53$ to illustrate the adequation of this fitting function. For comparison, the recovery curves in $\text{Na}_2\text{CsC}_{60}$ are also plotted, they are typical of recovery curves found in A_3C_{60} compounds^{38,39}. Here, the deviation from exponentiality is smaller, as illustrated by the value of the exponent for the stretched exponential ($\beta = 0.82$) closer to unity. The difference found for the exponent β for the two classes of systems indicates a significant difference in the relaxation curves and one can wonder whether it has a physical meaning.

In A_3C_{60} , the general belief^{38,39} is that the widely observed non-exponentiality is due to the differentiation between three slightly inequivalent ^{13}C sites on one C_{60} ball, when the motion of the balls is frozen. As the structure is much more different between Na_2C_{60} and K_4C_{60} than Na_2C_{60} and $\text{Na}_2\text{CsC}_{60}$, it seems unlikely that the change of relaxation behavior has a structural origin. We would rather suggest that it is related to a different nature of the relaxation in K_4C_{60} and Na_2C_{60} , more localized on the ball. Alternatively, this could be due to the addition of an extrinsic term caused by paramagnetic impurities.

B. Role of impurities in the low T relaxation

In insulating solids, as the intrinsic T_1 becomes long at low temperature, even a small number of paramagnetic impurities could become a dominant relaxation process. As a matter of fact, a rather high concentration of paramagnetic impurities seems to be always present in these compounds and their role in the low T relaxation must be considered. Paramagnetic impurities would likely produce a saturation of $1/T_1$ at low temperatures, i.e. an increase of $1/T_1T^{30}$. One could imagine that this “compensates” the decrease of the singlet-triplet component to mimic a $1/T_1T=\text{cst}$ law.

The comparison between Na_2C_{60} and K_4C_{60} can help to test whether this is likely. The paramagnetic contribution should have the same characteristics in both compounds but be proportional to the number of para-

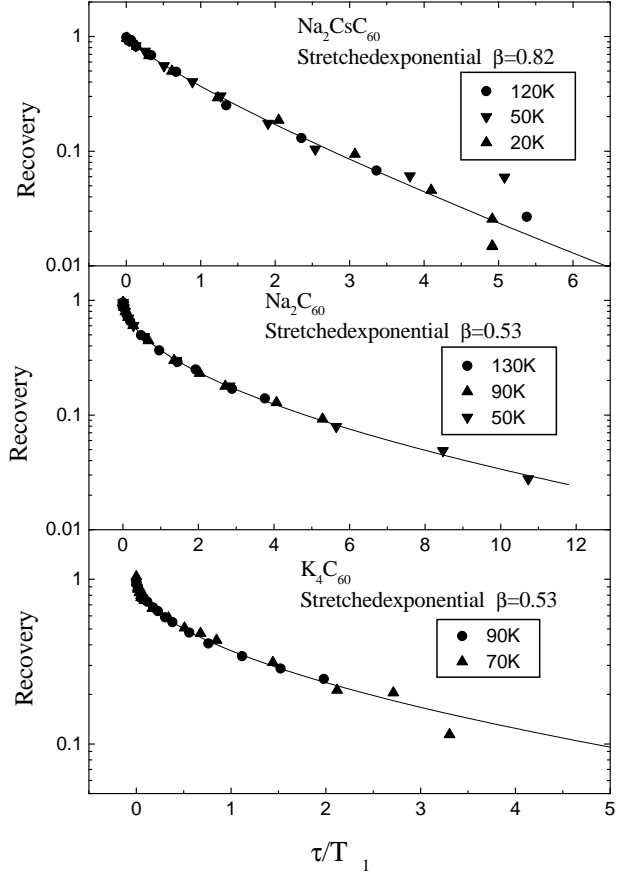


FIG. 13: Recovery curves for ^{13}C in $\text{Na}_2\text{CsC}_{60}$, Na_2C_{60} and K_4C_{60} , for different temperatures (see legend). $[M(\tau) - M_0] / M_0$ is plotted on a logarithmic scale, where $M(\tau)$ is the echo intensity at a delay τ after the saturation pulse and M_0 the intensity at saturation ($\tau \rightarrow \infty$). The recovery curves are scaled for the different temperatures by normalizing τ with the value of T_1 extracted from a stretched exponential fit with an exponent β indicated on the graph. The solid line is a fit to such a recovery law.

magnetic impurities in a given sample. We have characterized the paramagnetic impurity content by ESR on samples issued from the same batches as the NMR ones. From the low temperature Curie tail observed by ESR, the impurity concentrations are estimated to be about 2% per C_{60} in Na_2C_{60} and 1% in K_4C_{60} . We do observe longer T_1 in K_4C_{60} , but they are too long (by already a factor 10 at 70 K, as can be seen on Fig. 12) to be explained by a difference of a factor 2 in impurity content. Data in K_4C_{60} allow to set a maximal value for the contribution of impurities in Na_2C_{60} to $1/T_1T < 3 \cdot 10^{-4} (\text{sec K})^{-1}$ at 70 K, which is too small to be responsible for the deviation from the activated law.

Another independent indication of the intrinsic character of the relaxation comes from the fact that it is also observed by ^{23}Na NMR. As the increase of $1/T_1$ between 150 K and 300 K has very different magnitudes for ^{13}C and ^{23}Na , probably because a quadrupole term is present

in ^{23}Na $1/T_1$, it seems impossible that an intrinsic and extrinsic term could compensate at low T to give an identical temperature dependence on the two nuclei over a temperature range as large as 150 K.

We then conclude that our experiment probes a metallic character in Na_2C_{60} . As a proof of consistency, the value of $n(E_f)$ needed to explain the $1/T_1T=\text{cst}$ law by the Korringa mechanism can be estimated to be 1eV^{-1} , which agrees with the value of $\chi \approx 7.10^{-5}$ emu/mol found by ^{23}Na NMR¹¹.

V. CONCLUSION

In conclusion, the main properties of Na_2C_{60} and K_4C_{60} appear to be similar, which shows that they represent the typical behavior of two electrons or two holes in the t_{1u} band. Molecular excitations dominate their properties; starting from a singlet ground state, excitations to a triplet one are thermally accessible. We attribute the existence of these two states to the two most stable Jahn-Teller distortions, which have respectively a singlet and triplet ground state. We further show that this molecular approach is insufficient to describe the full temperature range. χ and $1/T_1$ seem to change more suddenly than one would expect in a completely thermal process. The structural transition from *fcc* to *sc* is not found essential in the variation of the properties of Na_2C_{60} . However, in both compounds, we evidence changes in the structure concomitant with the change in $1/T_1$, probably associated with the slowing down of molecular motions. This suggests that there is a coupling between the structure and the stabilization of JTD, maybe due to crystal field effects acting on the orbital moment of the different Jahn-Teller configurations.

We also give evidence that the singlet states are not strictly localized on one molecule. This is most clear by the low energy excitations observed in Na_2C_{60} at low temperatures, which are best described by a metallic-

like process with a small value of the density of states. Interactions between the balls also renormalize the value of the ST gap and yield to deviations with respect to a purely molecular model in the behavior of $1/T_1$ and χ .

The interplay between molecular and band-like properties is certainly one of the most intriguing feature of fullerides and a good understanding of this effect is a prerequisite before addressing the case of A_3C_{60} . The fact that these superconducting fullerides are surrounded by almost insulating phases has not always received much attention, probably because it is not easily possible to go from one phase to the other. When transport is measured as a function of alkali doping, usually on thin films or with the recently synthesized FET devices⁴⁰, no sharp metal to insulator transitions can be observed, which gives the impression that a rigid band filling picture could be applied. However, little is known on the homogeneity of the stoichiometries of these films and phase separation could take place there, like they do for bulk compounds. The well established fact that superconductivity is restricted to a very limited doping range around $n=3$ is a strong deviation from the expectations of a BCS theory usually applied to these materials. This indicates particular properties for the *integer filling* $n=3$. This might also be true for $n=2$ and 4, and the metallic state could be nearly suppressed *only* in these two cases. This importance of integer fillings might be related to the stronger correlation effects that appear in this case combined with the possibility of stabilizing molecular JTD. On one hand, the case of Na_2C_{60} studied here indicates that metallic and molecular properties are not exclusive but *do* coexist. On the other hand, the study of CsC_{60} that we will present in paper II shows that JTD C_{60}^{2-} have an enhanced stability in this compound with nominally one electron per C_{60} . We will develop in paper III the idea that the remarkable properties of A_3C_{60} are due to an optimum cooperation between metallic and molecular aspects, because of its symmetric position between $n=2$ and 4.

¹ S.C. Erwin, in *Buckminsterfullerenes*, edited by W.E. Billups and M.A. Ciufolini (VCH, New York, 92)

² R.F. Kiefl *et al.*, *Phys. Rev. Lett.* **69**, 2005 (92)

³ P. Petit *et al.*, *Progress in Fullerene research*, World scientific, edited by H. Kuzmany, J. Fink, M. Mehring and S. Roth, p.148 (94)

⁴ I. Lukyanchuk, N. Kirova, F. Rachdi, C. Goze, P. Molinie and M. Mehring *Phys. Rev. B* **51**, 3978 (95)

⁵ G. Zimmer, M. Helme, M. Mehring and F. Rachdi, *Euro-physics Letters* **27**, 543 (94)

⁶ G. Zimmer, M. Mehring, C. Goze and F. Rachdi, *Phys. Rev. B* **52**, 13 300 (95)

⁷ R. Kerkoud, P. Auban-Senzier, D. Jerome, S. Brazovskii, I. Luk'yanchuk, N. Kirova, F. Rachdi, and C. Goze *J. Phys. Chem. Solids* **57**, 143 (96)

⁸ R. Hesper, L.H. Tjeng, A. Heeres and G.A. Sawatzky *Phys. Rev. B* **62**, 16046 (00) and references therein

⁹ Y. Iwasa and T. Kaneyasu *Phys. Rev. B* **51**, 3678 (95)

¹⁰ M. Knupfer and J. Fink, *Phys. Rev. Lett.* **79**, 2714 (97)

¹¹ V. Brouet, H. Alloul, L. Thien-Nga, S. Garaj and L. Forró, *Phys. Rev. Lett.* **86**, 4680 (01)

¹² O. Zhou and D. Cox, *J. Phys. Chem. Solids* **53**, 1373 (92)

¹³ C.A. Kuntscher, G.M. Bendele and P.W. Stephens *Phys. Rev. B* **55**, R3366 (97)

¹⁴ G. Oszlanyi, G. Baumgartner, G. Faigel, L. Granasy and L. Forró, *Phys. Rev. B* **58**, 5 (98)

¹⁵ O. Gunnarsson, S.C. Erwin, E. Koch and R. M. Martin *Phys. Rev. B* **57**, 2159 (1998); J. E. Han, E. Koch and O. Gunnarsson, *Phys. Rev. Lett.* **84**, 1276 (00)

¹⁶ T. Yildirim, J. E. Fischer, A. B. Harris, P. W. Stephens, D. Liu, L. Brard, R. M. Strongin, and A. B. Smith, *Phys. Rev. Letters* **71**, 1383 (93)

¹⁷ V. Brouet, H. Alloul and L. Forró, in preparation

¹⁸ V. Brouet, H. Alloul, S. Garaj and L. Forró, in preparation

- ¹⁹ N. Manini, E. Tosatti and A. Auerbach *Phys. Rev. B* **49**, 13008 (94)
- ²⁰ M. Fabrizio and E. Tosatti, *Phys. Rev. B* **55**, 13 465 (97)
- ²¹ M. Capone, M. Fabrizio, P. Giannozzi and E. Tosatti, *Phys. Rev. B* **62**, 7619 (00)
- ²² C.H. Pennington and V.A. Stenger, *Reviews of modern physics*, **68**, 855 (96)
- ²³ R. Tycko, G. Dabbagh, R.M. Fleming, R.C. Haddon, A.V. Makhija and S.M. Zahurak, *Phys. Rev. Lett.* **67**, 1886 (91)
- ²⁴ J. Reichenbach *et al.*, *J. Chem. Physics*, **101**, 4585 (94)
- ²⁵ R. Tycko, G. Dabbagh, M.J. Rosseinsky, D.W. Murphy, A.P. Ramirez, R.M. Fleming, *Phys. Rev. Letters* **68**, 1912 (92)
- ²⁶ C.P. Slichter, *Principles of Magnetic Resonance*, Springer-Verlag (90)
- ²⁷ Y. Yoshinari, H. Alloul, G. Kriza and K. Holczer, *Phys. Rev. Lett.* **71**, 2413 (93)
- ²⁸ N. Bloembergen, E.M. Purcell and R.V. Pound, *Phys. Rev.* **73**, 679 (48)
- ²⁹ Y. Yoshinari, H. Alloul, V. Brouet, G. Kriza, K. Holczer and L. Forro, *Phys. Rev. B* **54**, 6155 (96)
- ³⁰ A. Abragam, *Principle Of Nuclear Magnetism*, Oxford University Press (61)
- ³¹ R.D. Johnson, C.S. Yannoni, H.C. Dorn, J.R. Salem and D.S. Bethune, *Science* **255**, 1235 (92)
- ³² A. Pénicaud *et al.*, *in preparation*
- ³³ P. Launois, R. Moret, N.R. de Souza, J.A. Azamar-Barrios and A. Pénicaud, *Eur. Phys. Journal B* **15**, 445 (00)
- ³⁴ T. Yldirim, J.E. Fischer, R. Dinnebier, P.W. Stephens and C.L. Lin *Solid State Communication* **93**, 26 (95)
- ³⁵ K. Prassides, C. Christides, I.M. Thomas, J. Mizuki, K. Tanigaki, I. Hirosawa, T.W. Ebbesen, *Science* **263**, 950 (94)
- ³⁶ V.Brouet, H. Alloul, T. Saito and L. Forro in *Electronic Properties of Novel MaterialsMolecular Nanostructure*, edited by H. Kuzmany, J. Fink, M. Mehring, and S. Roth, AIP Conf. Proc. No. **544** (AIP, New York, 2000), p. 24.
- ³⁷ K. Kamaras, G. Klupp, D.B. Tanner, A.F. Hebard, N.M. Nemes and J.E. Fischer, *to be published*
- ³⁸ K. Holczer, O. Klein, H. Alloul, Y. Yoshinari, F. Hippert, S.-M. Huang, R.B. Kaner and R.L. Whetten, *Europhysics Letters*, **23**, 63 (1993)
- ³⁹ Y. Maniwa *et al.*, *Journal of the physical society of Japan*, **63**, 1139 (1994)
- ⁴⁰ J.H. Schon, Ch. Kloc, R.C. Haddon and B. Batlogg, *Science* **288**, 656 (2000)